



1 **Title:** Elephant megacarcasses increase local nutrient pools in African savanna soils and plants

2

3 Courtney G. Reed<sup>1\*</sup>, Michelle L. Budny<sup>2</sup>, Johan T. du Toit<sup>3,4</sup>, Ryan Helcoski<sup>3</sup>, Joshua P.

4 Schimel<sup>1</sup>, Izak P. J. Smit<sup>5,6</sup>, Tercia Strydom<sup>5</sup>, Aimee Tallian<sup>3,7</sup>, Dave I. Thompson<sup>8,9</sup>, Helga van

5 Coller<sup>8,10</sup>, Nathan P. Lemoine<sup>2,11</sup>, Deron E. Burkepile<sup>1,8\*</sup>

6

7 <sup>1</sup>Department of Ecology, Evolution, and Marine Biology, University of California, Santa

8 Barbara, CA, USA

9 <sup>2</sup>Department of Biological Sciences, Marquette University, Milwaukee, WI, USA

10 <sup>3</sup>Department of Wildland Resources, Utah State University, Logan, UT, USA

11 <sup>4</sup>Institute of Zoology, Zoological Society of London, London, England, UK

12 <sup>5</sup>Scientific Services, South African National Parks, Skukuza, South Africa

13 <sup>6</sup>Sustainability Research Unit, Nelson Mandela University, George, South Africa

14 <sup>7</sup>Norwegian Institute for Nature Research, Høgskoleringen 9 Trondheim, 7485 Norway

15 <sup>8</sup>South African Environmental Observation Network (SAEON), Ndlovu Node, Phalaborwa,

16 South Africa

17 <sup>9</sup>Unit for Environmental Sciences and Management, Potchefstroom Campus, North West

18 University, Potchefstroom, South Africa

19 <sup>10</sup>The Expanded Freshwater and Terrestrial Environmental Observation Network (EFTEON),

20 Kimberley 8306, South Africa

21 <sup>11</sup>Department of Zoology, Milwaukee Public Museum, Milwaukee, WI, USA

22

<https://doi.org/10.5194/egusphere-2024-1514>

Preprint. Discussion started: 30 May 2024

© Author(s) 2024. CC BY 4.0 License.



23 \*Corresponding authors: Courtney Reed, [courtneyreed@ucsb.edu](mailto:courtneyreed@ucsb.edu), Deron Burkepile,

24 [dburkepile@ucsb.edu](mailto:dburkepile@ucsb.edu)



25 **Abstract**

26 African elephants (*Loxodonta africana*) are the largest extant terrestrial mammals, with bodies  
27 containing enormous quantities of nutrients. Yet we know little about how these nutrients move  
28 through the ecosystem after an elephant dies. Here, we investigated the initial effects (1-26  
29 months post-death) of elephant megacarcasses on savanna soil and plant nutrient pools in Kruger  
30 National Park, South Africa. We hypothesized that: (H1) elephant megacarcass decomposition  
31 would release nutrients into soil, resulting in higher concentrations of soil nitrogen (N),  
32 phosphorus (P), and micronutrients near the center of carcass sites; (H2) carbon (C) inputs to the  
33 soil would stimulate microbial activity, resulting in increased soil respiration potential near the  
34 center of carcass sites; and (H3) carcass-derived nutrients would move from soil into plants,  
35 resulting in higher foliar nutrient concentrations near the center of carcass sites. To test our  
36 hypotheses, we identified 10 elephant carcass sites split evenly between nutrient-poor granitic  
37 and nutrient-rich basaltic soils. At each site, we ran transects in the four cardinal directions from  
38 the center of the gravesite, collecting soil and grass (*Urochloa mosambicensis*) samples at 0, 2.5,  
39 5, 10, and 15 m. We then analyzed samples for CNP and micronutrient concentrations and  
40 quantified soil microbial respiration potential. We found that concentrations of soil nitrate,  
41 ammonium,  $^{15}\text{N}$ , P, sodium, and potassium were elevated closer to the center of carcass sites  
42 (H1). Microbial respiration potentials were positively correlated with soil organic C, and both  
43 respiration and organic C decreased with distance from the carcass (H2). Finally, we found  
44 evidence that plants were readily absorbing carcass-derived nutrients from the soil, with foliar  
45 %N,  $^{15}\text{N}$ , iron, potassium, and sodium significantly elevated closer to the center of carcass sites  
46 (H3). Together, these results indicate that elephant megacarcasses release ecologically  
47 consequential pulses of nutrients into the soil, which then move into above-ground nutrient pools

<https://doi.org/10.5194/egusphere-2024-1514>

Preprint. Discussion started: 30 May 2024

© Author(s) 2024. CC BY 4.0 License.



48 in plants. These localized nutrient pulses may drive spatiotemporal heterogeneity in plant

49 diversity, herbivore behavior, and ecosystem processes.



50 **Sect. 1 Introduction**

51 Living animals affect nutrient flows and ecosystem processes (Schmitz et al. 2018), but we have  
52 only recently acknowledged that animal carcasses could also influence nutrient availability  
53 (Barton et al. 2013; Monk et al. 2024). In marine ecosystems, whale carcasses function as unique  
54 hotspots of nutrient cycling, biodiversity, and ecosystem processes (Roman et al. 2014). In  
55 terrestrial systems, mass mortality events (e.g., wildebeest, cicadas) create nutrient hotspots  
56 (Yang, 2004; Subalusky et al. 2020), while individual small and medium-sized carcasses release  
57 pulses of nutrients into the soil (Town, 2000; Barton et al. 2016; Olea et al. 2019). Yet, terrestrial  
58 ecosystem ecology lacks knowledge about another potential driver of spatiotemporal  
59 heterogeneity in nutrient cycling and ecosystem processes – megacarcasses (animals such as  
60 elephants and rhinoceros that are >1000 kg at death) – which may be functionally different than  
61 smaller carcasses due to the extraordinarily high concentration of nutrients and residence time of  
62 the decomposing animal (see reviews by Barton et al. 2013; Barton, 2016; Barton & Bump  
63 2019). This question is particularly relevant given the megaherbivore losses that occurred during  
64 the Pleistocene extinctions and that are still occurring today (Ripple et al. 2015). We are only  
65 beginning to understand how the ‘extinction aftershock’ of losing the largest species impacts  
66 ecosystems (Owen-Smith, 1989; Flannery, 1990), and no study has yet investigated how the loss  
67 of megacarcasses might influence terrestrial ecosystem dynamics (Doughty et al. 2013; Doughty  
68 et al. 2016).

69 We can only evaluate the importance of terrestrial megacarcasses for nutrient cycling in  
70 ecosystems where megaherbivores still exist, such as African savannas. The African savanna  
71 elephant (*Loxodonta africana*) is the largest extant land animal and is known for its key  
72 ecological effects in savannas while alive (e.g., dispersing seeds, creating plant refuges,



73 preventing woody encroachment) (Skarpe et al. 2004; Asner et al. 2009; Campos-Arceiz &  
74 Blake, 2011; Coverdale et al. 2016; Guy et al. 2021). The elephant's large body mass may mean  
75 that it also has an outsized impact after death. A 4000-kg elephant megacarcass likely represents  
76 ~2000 kg carbon (C), ~300 kg nitrogen (N), and ~125 kg phosphorus (P) deposited in the  
77 savanna landscape (estimated from stoichiometry of elephants and other mammals in Sterner &  
78 Elser, 2002). The N deposition from one elephant megacarcass (in a 700 m<sup>2</sup> impact zone  
79 assuming a 15 m disturbance radius) is roughly equivalent to the N delivered to 10,000 m<sup>2</sup> of  
80 savanna from ~100 years from atmospheric deposition (Mphepya et al. 2006).

81         If megacarcasses provide large nutrient pulses, then they likely create hotspots of  
82 important below- and aboveground processes. Belowground, soil respiration and organic matter  
83 decomposition might increase with nutrient inputs from carcasses (Rische et al. 2020).  
84 Concentrations of C, N, P, and potassium (K) are elevated near carcasses of medium-sized  
85 animals (e.g., bison, moose, kangaroo, vicuña) (Towne, 2000; Bump et al. 2009a; Macdonald et  
86 al. 2014; Risch et al. 2020; Monk et al. 2024), and nutrients such as P and calcium (Ca) continue  
87 leaching from bones even after soft tissues have been consumed or degraded (Coe, 1978; Keenan  
88 & Beeler, 2023). Aboveground, plant growth in African savannas is strongly limited by nutrient  
89 availability, most commonly N and P, but also by micronutrients such as Ca, K, and magnesium  
90 (Mg) (Jobbágy & Jackson, 2004; Ries & Shugart, 2008; Pellegrini, 2016). Thus, the large influx  
91 of nutrients released from megacarcasses might increase the mobilization of nutrients by plants,  
92 potentially increasing nutrient accessibility for above-ground herbivores (Yang, 2008; Grant &  
93 Scholes, 2006; Anderson et al. 2010; Joern et al. 2012). Indeed, carcasses of smaller vertebrates  
94 (e.g., salmon, deer) can increase the proportions of nitrogen and <sup>15</sup>N in plants within just a few  
95 months post-death (Hocking & Reynolds, 2012; van Klink et al. 2020).



96 To assess the effects of megacarcasses on local nutrient pools (Figure 1), we measured  
97 the initial contributions of elephant carcasses (1-26 months post-death) to soil and plant nutrients  
98 in the Kruger National Park (KNP), South Africa. Further, we examined the effects of elephant  
99 carcasses on the two main soil types in KNP: sandy, relatively nutrient-poor granitic soils and  
100 clayey, nutrient-rich basaltic soils (Venter et al. 2003). At each site, we ran transects in each  
101 cardinal direction from the center of the site where an elephant died, collecting samples of soil  
102 and a palatable grass species (*Urochloa mosambicensis*) at 0, 2.5, 5, 10, and 15 m. We then  
103 analyzed soil samples for C<sub>NP</sub> content, quantified soil microbial respiration potential, and  
104 measured %N and <sup>15</sup>N in grass tissue. We hypothesized that: (H1) elephant megacarcass  
105 decomposition would release nutrients into soil, resulting in higher concentrations of soil N, P,  
106 and micronutrients near the center of carcass sites; (H2) C inputs to the soil would stimulate  
107 microbial activity, resulting in increased soil respiration potential near the center of carcass sites;  
108 and (H3) carcass-derived nutrients would move from soil into plants, resulting in higher foliar  
109 nutrient concentrations near the center of carcass sites. We predicted that enrichment effects  
110 from megacarcasses would be greater on nutrient-poor granitic sites compared to nutrient-rich  
111 basaltic sites.

112

## 113 **Sect. 2 Methods**

### 114 **2.1 Study system and sample collection**

115 We performed this research in the southern part of the Kruger National Park (KNP), South  
116 Africa (24.996 S, 31.592 E, ~275m elevation). The landscape is a mix of savanna grasslands and  
117 broadleaf woodlands, with an overstory dominated by trees from the genus *Combretum* (red  
118 bushwillow, *C. apiculatum*; russet bushwillow, *C. hereroense*; leadwood, *C. imberbe*) and trees



119 formerly known as acacias (knobthorn, *Senegalensis nigrescens*; umbrella thorn, *Vachellia*  
120 *tortillis*). The park hosts a full suite of African savanna animals, including ~30,000 elephants  
121 (*Loxodonta africana*) (Coetsee & Ferreira, 2023), with a mortality rate of ~2% (~600 elephants  
122 per year). The targeted region of KNP has a high density of scavengers and predators, including  
123 white-backed vultures (*Gyps africanus*), spotted hyenas (*Crocuta crocuta*), and lions (*Panthera*  
124 *leo*) (Owen-Smith & Mills, 2007).

125       During the wet season in March 2023, we identified ten elephant carcass sites (1-26  
126 months post-death), five on relatively nutrient-rich basaltic soil and five on nutrient-poor granitic  
127 soil. KNP section rangers provided precise GPS locations of where elephant carcasses had been  
128 found. These sites were recognizable *in situ* by a persistent bonefield, undigested gut contents,  
129 and an absence of herbaceous vegetation. At each site, we hammered a rebar post into the center  
130 of the megacarcass disturbance and ran 15 m transects out from the post in each of the four  
131 cardinal directions. We collected green leaf material from *Urochloa mosambicensis*, a common  
132 and abundant palatable grass species, and used an auger to collect soil samples to a depth of 10  
133 cm at five points along each transect (0.5, 2.5, 5, 10, and 15 m). We pooled and homogenized the  
134 samples to yield one composite leaf and one composite soil sample per sampling distance from  
135 each carcass site. Soil samples were sieved in a 5-mm metal sieve which was cleaned in between  
136 samples with 70% ethanol. On the day of collection, we used 5 g of each soil sample for soil  
137 respiration measurements (described below). The rest of each sample was stored plastic bags in a  
138 -20°C freezer until nutrient analyses. Leaf samples were stored in paper bags at room  
139 temperature until dried for analyses (see below).

140

### 141 **2.3 Hypothesis testing**





142 We tested our first hypothesis that elephant megacarcass decomposition would release nutrients  
143 into the soil by performing soil nutrient analyses. First, we sent 250 g of each soil sample to Eco-  
144 Analytica laboratory at the North-West University in Potchefstroom, South Africa for  
145 measurements of soil ion concentrations of ammonium  $[\text{NH}_4]^+$ , nitrate  $[\text{NO}_3]^-$ , phosphate  $[\text{PO}_4]^{3-}$ ,  
146 and plant-available P using a 1:2 water extract analysis. To determine whether soil  
147 micronutrients were distinct and elevated at the center of carcass sites relative soil further from  
148 the center, Eco-Analytica used mass spectrometry to measure concentrations of sodium (Na),  
149 magnesium (Mg), iron (Fe), calcium (Ca), and potassium (K), which are micronutrients  
150 important to both plant reproduction and herbivore nutrition (Pandey, 2010; Chen et al. 2015; Hu  
151 et al. 2021; Kaspari, 2021; Sardans & Peñuelas, 2021). Finally, to determine whether elevated N  
152 levels in soils were derived from the carcass, we sent 10 g of each sample to the BIOGRIP  
153 laboratory within the Central Analytical Facility at Stellenbosch University for measurements of  
154 soil %N and  $^{15}\text{N}$ , obtained using a Vario Isotope Select Elemental Analyzer connected to a  
155 thermal conductivity detector and an Isoprime precision isotope ratio mass spectrometer (IRMS).

156 To test our second hypothesis that nutrient inputs to the soil would stimulate microbial  
157 activity, we measured soil organic C, water content, and microbial respiration potential. We sent  
158 10 g of each sample to the BIOGRIP laboratory for measurements of soil organic C using a  
159 Vario TOC Cube (Elementar, Langensfeld, Germany). To quantify soil respiration and water  
160 content, we used an incubation method (Lemoine et al. 2024) in which 5 g ( $\pm 0.2$  g) of each  
161 sample was placed into a 100 ml clear glass bottle, sealed, and flushed with  $\text{CO}_2$ -free air.  
162 Following flushing, we incubated the bottles for one hour at  $25^\circ\text{C}$ . We then recorded  $\text{CO}_2$   
163 concentrations using an LI-850  $\text{CO}_2/\text{H}_2\text{O}$  infrared gas analyzer. After soil respiration  
164 measurements, we determined sample dry weight by drying each sample at  $60^\circ\text{C}$  for 24-48 hours



165 until stable mass was achieved. We subtracted dry weight from starting weight to obtain soil  
166 water content. Finally, we used the dry weights and the Ideal Gas Law to standardize all  
167 respiration measurements to  $\text{CO}_2 \mu\text{g h}^{-1}\text{g dry soil}^{-1}$ .

168 To test our third hypothesis that carcass-derived nutrients would move from soil into  
169 plants, we measured foliar nutrient concentrations in *U. mosambicensis*. We dried each leaf  
170 sample in a drying oven at  $60^\circ\text{C}$  for 48 hours, ground dried samples with a Retsch MM400 mill  
171 (Germany), and sent 2 g of each dry sample to the BIOGRIP laboratory for measurements of %N  
172 and  $^{15}\text{N}$  via stable isotope analysis as described above. Additionally, we sent 5 g per sample to  
173 Cedara Analytical Services Laboratory to quantify micronutrients in grass tissue (P, Na, Mg, K,  
174 Ca, and Fe) using a microwave-assisted digestion procedure (Ethos UP, Magna Analytical) and  
175 an Agilent ICP-MS mass spectrometer. At three of the ten sites, we did not find sufficient plant  
176 material at the central point for analysis, resulting in a sample size of  $N = 7$  for the center  
177 (distance = 0-0.5m) measurement for leaf nutrient analyses.

178 To test whether each response variable for the three hypotheses was significantly  
179 associated with soil type and/or distance from the carcass center, we performed a model selection  
180 procedure. For each response variable, we first ran a Shapiro-Wilk normality test to determine  
181 whether the variable was normally distributed. If not, we normalized the data via log-  
182 transformation, adding 0.001 to each variable before transformation to address zeros in the  
183 dataset. Soil %N, nitrate, ammonium,  $^{15}\text{N}$ , phosphate, plant-available P, organic C, respiration,  
184 water, and micronutrients were non-normally distributed and required log transformations  
185 (Figure S1). Leaf micronutrients were normally distributed except for Fe and Ca (Figure S2),  
186 which we log-transformed for individual analysis. Next, we ran five generalized linear mixed  
187 models in the package *lme4* (Bates et al. 2015) for each response variable: (i) soil type + distance



188 + soil type  $\times$  distance interaction, (ii) soil type + distance, (iii) soil type, (iv) distance, and (v) a  
189 null model indicating no significant difference in slope or intercept after accounting for carcass  
190 site. All models included carcass site as a random effect to account for individual variation. The  
191 narrow distribution of ages (1-26 months since death) with the sample size of  $N = 10$  sites made  
192 testing for the effect of age challenging, so we did not include carcass age in the models. We  
193 compared the models for each response variable using Akaike Information Criterion (AICc).  
194 Models with a  $\Delta\text{AICc} \leq 2$  were considered roughly equivalent in fit (Burnham and Anderson,  
195 2002).

196 In addition to these models, for our second hypothesis we regressed soil respiration  
197 potential against soil organic C, expecting that the two would be positively correlated. We ran a  
198 generalized linear mixed model with soil respiration potential as the response variable. The  
199 model included soil organic C + distance + soil type, with carcass site as a random effect. We did  
200 not include an interaction with soil type in this model due to sample size restrictions. Respiration  
201 potential and organic C were both log-transformed to achieve normality.

202 To determine whether leaf and soil micronutrient composition differed with distance and  
203 soil type, we ran permutational analysis of variance (perMANOVA) in *vegan* (Oksanen et al.  
204 2022). We ran the same model separately for soil and leaf micronutrient composition (soil type +  
205 distance). To determine which micronutrients contributed most to compositional differences  
206 across distances and soil types, we calculated samplewise Bray-Curtis dissimilarity and  
207 performed principal component analysis. Finally, we ran linear models to test for correlations  
208 between leaf and soil concentrations of each micronutrient. Each model included distance as a  
209 covariate and site as a random effect.

210 All statistical analyses were performed in R version 4.2.1 (R Core Team, 2022).



211

## 212 **Sect. 3 Results**

### 213 **3.1 Hypothesis 1: Effects of megacarcasses on soil nutrient pools**

214 We found partial support for our first hypothesis that soil N and P concentrations would be  
215 higher closer to the center of carcass sites (Table S1). Our results were inconclusive for soil %N  
216 (Figure 2A) and nitrate concentration (Figure 2B); there was substantial support for the null  
217 model and an alternative model in both instances. For %N, soil type was the top model, with %N  
218 higher in basaltic soils, but there was also some support for the null model ( $\Delta\text{AICc} = 1.80$ ). The  
219 top model for soil nitrate was distance and showed nitrate decreasing with distance from the  
220 center of the carcass site, but the null model also had some support in this case as well ( $\Delta\text{AICc} =$   
221 1.68). The top model for ammonium concentration (Figure 2C) was soil type + distance,  
222 indicating that ammonium concentrations were greatest in granitic soils and decreased with  
223 distance from the carcass regardless of soil type. The top models for  $^{15}\text{N}$  (Figure 2D) were (i)  
224 distance and (ii) soil + distance.  $^{15}\text{N}$  was greatest in granitic soils and decreased with distance  
225 regardless of soil type, indicating that the proportion of animal-sourced N was greater near the  
226 center of the carcass site. The top model for phosphate (Figure 2E) was soil type + distance +  
227 soil type  $\times$  distance interaction. Phosphate concentrations were greater in granitic soils, but only  
228 towards the center of carcass sites. Phosphate concentrations dropped precipitously from 0-2.5 m  
229 distance and then were similar in both soil types. For plant-available P (Figure 2F), all four  
230 biological models (excluding the null) fell within the set of top models. Plant-available P was  
231 greater in basaltic soils and decreased with distance from the center in both soil types, but the  
232 effect of distance was stronger in granitic soils.



233 Contrary to our first hypothesis, soil micronutrient composition did not differ  
234 significantly with distance from the carcass center; nor did most individual micronutrients (Table  
235 S1). The perMANOVA results showed that soil micronutrient composition did not differ  
236 significantly with distance ( $R^2 = 0.00$ ,  $F_{4,44} = 0.1$ ,  $P = 1.000$ ) (Figure S3A), but it did differ  
237 significantly with soil type ( $R^2 = 0.71$ ,  $F_{1,44} = 108.8$ ,  $P = 0.001$ ) (Figure S3B). Principal  
238 components analysis showed that dimension 1 explained 53.6% of the variation between soil  
239 types and was driven primarily by differences in Mg, Ca, and Fe. Dimension 2 explained 25.9%  
240 of variation and was driven primarily by differences in K. The top model for Na (Figure S4A)  
241 was distance, indicating a significant decrease in soil Na with distance from the carcass. The top  
242 model for K (Figure S4B) was soil type + distance + soil type  $\times$  distance interaction. Soil K was  
243 greater in basaltic soils and decreased with distance only in granitic soils. The remaining three  
244 micronutrients (Ca, Fe, and Mg) all had soil type as the top model, appearing in higher  
245 concentrations in basaltic soils (Figure S4C-E).

246

### 247 **3.2 Hypothesis 2: Effects of megacarcasses on soil carbon and respiration**

248 Consistent with our second hypothesis, soil respiration potential was positively correlated with  
249 soil organic carbon concentration ( $P = 0.039$ ) and decreased significantly with distance ( $P =$   
250  $0.020$ ) but did not differ with soil type ( $P = 0.408$ ) (Figure 3). Results for soil water content  
251 (Figure S5) were inconclusive. The top model for water was soil, showing higher water content  
252 in granitic soils, but there was also strong support for the null model ( $\Delta AICc = 0.42$ ).

253

### 254 **3.3 Hypothesis 3: Effects of megacarcasses on plant nutrient pools**



255 Consistent with our third hypothesis, we found evidence that N from carcasses had moved from  
256 soils into plants. Leaf %N (Figure 4A) and  $^{15}\text{N}$  (Figure 4B) both decreased significantly with  
257 distance from the carcass site, indicating that the high N content in leaves closer to the center of  
258 a megacarcass site likely had an animal origin. These trends did not hold true for P (Figure 4C),  
259 another major limiting nutrient for savanna plants; the top model for leaf P was the null,  
260 indicating no difference in leaf P content with soil type or distance from the carcass (Figure 4C).

261 Leaf micronutrient composition did not differ significantly with distance ( $R^2 = 0.08$ ,  $F_{4,40}$   
262  $= 1.7$ ,  $P = 0.115$ ; Figure S6A) but did differ with soil type ( $R^2 = 0.43$ ,  $F_{1,40} = 34.7$ ,  $P = 0.001$ ;  
263 Figure S6B). Dimension 1 explained 44.4% of the variance across soil types and was primarily  
264 driven by Mg and Na. Dimension 2 explained 30.0% of the variance and was driven mainly by  
265 Ca. The top model for Na (Figure 5A) was soil type by distance, showing that leaf Na decreased  
266 with distance and was greater in basaltic soils. Leaf K (Figure 5B) and Fe (Figure 5C) both had  
267 distance as the top model and decreased significantly with distance from the carcass. The top  
268 models for Ca (Figure 5D) and Mg (Figure 5E) were the nulls, indicating no significant  
269 difference in these nutrients with distance or soil type. However, none of the individual  
270 micronutrients were correlated between soil and leaf samples (Table S3).

271

#### 272 **Sect. 4 Discussion**

273 Here, we show that elephant megacarcasses influence soil and foliar nutrients during at least the  
274 first two years following mortality. Consistent with our hypotheses, soil nitrate (Figure 2B),  
275 ammonium (Figure 2C),  $^{15}\text{N}$  (Figure 2D), and P (Figure 2E-F) concentrations were all elevated at  
276 the center of carcass sites and decreased with distance from the center. Microbial respiration  
277 potential was also elevated towards the center of carcass sites and was strongly correlated with



278 the influx of organic C (Figure 3A). Finally, %N (Figure 4A) and <sup>15</sup>N in grass (Figure 4B) were  
279 both elevated closer to the centers of carcass sites compared to grass farther from carcasses.  
280 Similarly, micronutrients Na and K in both soils and grasses were elevated closer to the center of  
281 carcass sites. Together, these results indicate that carcass-derived nutrients move into soil and  
282 subsequently into plants over relatively short time scales, cycling essential nutrients such as N  
283 from carrion into the soil and back into aboveground nutrient pools.

284 The initial influx of ammonium from elephant carcasses is consistent with literature on  
285 smaller carrion (Parmenter & McMachon, 2009; Quaggiotto et al. 2019; Yong et al. 2019). The  
286 mean ammonium level at the center of carcass sites (17.4 mg/L) was 5x the level generally  
287 considered toxic to plants (3.5 mg/L; Britto & Kronzucker, 2002). Yet, we found living grass—  
288 typically *Urochloa mosambicensis*—in the center of the carcass site at seven out of ten of our  
289 sites and at the 2.5m distance for all sites. The three sites without vegetation in the center had the  
290 highest ammonium levels (35-72 mg/L), suggesting that *U. mosambicensis* has a higher degree  
291 of ammonium tolerance than some sympatric grass species but may still be limited by the  
292 extreme ammonium levels at the centers of these three relatively fresh carcass sites. These results  
293 indicate that ammonium remains elevated at elephant carcass sites for at least the first two years  
294 post-death and may reduce, but not eliminate, plant growth over this time period.

295 Soil nitrate (Figure 2B) and soil respiration potential (Figure 3A) were also elevated near  
296 the center of carcass sites, implying that the higher rates of soil microbial biomass and activity  
297 are resulting in the oxidation of ammonium to nitrate (Prosser, 2011). These results are  
298 consistent with other work on carrion, where microbial activity tends to be greater in soils near  
299 carcasses as compared to surrounding soil (Bump et al. 2009b). However, carcass effects on soil  
300 microbial respiration exhibit a high degree of intra-system variation (elk, bison; Risch et al.



301 2020), and the potentially short window during which increased respiration occurs may make  
302 capturing these variations challenging. For example, soil respiration potential at the center of the  
303 three youngest carcass sites was on average 2x higher than the seven older sites (18.43 and 9.62  
304  $\mu\text{gCO}_2/\text{hr}$ , respectively). Thus, the impact of increased organic C on soil microbial processes  
305 may be relatively short lived and last a matter of months.

306 Elevated soil phosphate (Figure 2E) and plant-available P (Figure 2F) at the center of  
307 carcass sites were also consistent with expectations from the literature (Bump et al. 2009a;  
308 Parmenter & MacMahon, 2009). However, elevated P levels in soil did not translate to elevated  
309 P in grass leaves (Figure 4C), which could suggest a lag between trends in soil and plants that is  
310 longer for P than for N. This lag could occur because P has low water solubility relative to N and  
311 therefore is less mobile in soils (Wiersum, 1962).

312 The elevated plant-available P at the center of carcass sites likely came primarily from  
313 phosphate released from decomposing tissue (Yong et al. 2019). Bone decomposition occurs  
314 over years (Coe, 1978) and therefore should result in the slow release of P and a gradual decrease  
315 in the N:P ratio (Parmenter & MacMahon, 2009; Quaggiotto et al. 2019). Indeed, initial  
316 inorganic N influxes to the Mara River in Kenya from mass wildebeest die-offs are 10-fold  
317 greater than concurrent increases in P, which instead releases slowly over about seven years of  
318 bone decomposition (Subalusky et al. 2017). Research following megacarcasses over longer  
319 timeframes post-death is needed to clarify when P from enriched soil moves into plants and at  
320 what stage megacarcass bones begin contributing to soil P dynamics. It is also possible that bone  
321 dispersal by scavengers may result in the P leaching from bones at distances far from the carcass  
322 site, reducing their local effects at sites of elephant mortality.





323           The contributions of megacarcasses to soil nutrient pools were strongly associated with  
324 soil type. Results confirmed that basaltic soils are overall more nutrient rich, with greater  
325 concentrations of micronutrients (P, Ca, Fe, and Mg; Figure S4B-E). However, soil ammonium  
326 (Figure 2C) and phosphate (Figure 2E) concentrations were both greater in granitic soils,  
327 indicating that organic matter from megacarcasses may persist longer in nutrient-poor and sandy  
328 granitic soil compared with nutrient-rich and clayey basaltic soil. With the exception of Na  
329 (Figure 5A), soil type had no significant effect on leaf micronutrient concentrations (Figure 5B-  
330 E). We were surprised that grass on more nutrient-rich soil did not exhibit greater nutrient  
331 concentrations. One potential explanation is that grass may primarily be limited by  
332 macronutrients like N and P on both soil types (Craine et al. 2008; Holdo, 2013) rather than by  
333 micronutrients. Thus, even with increased micronutrient availability their actual uptake may not  
334 differ substantially. Studies on ungulate carcasses (e.g., muskoxen, moose, zebra) have shown  
335 increased foliar N at carcass sites (Danell et al. 2002; Bump et al. 2009b; Turner et al. 2014), but  
336 to date there is little research on the flow of micronutrients from carrion to plants and none on  
337 the pipeline from megacarcasses to plants. Moreover, it remains to be seen whether increases in  
338 foliar N and other nutrients affect herbivory rates at carcass sites and how long such effects may  
339 last.

340

## 341 **Sect. 5 Conclusions**

342 This research is an initial step in understanding the ecological legacies of megacarcasses on  
343 savanna nutrient pools. During the first two years post-death, megacarcasses released pulses of  
344 N, P, and key micronutrients, which all influence primary production when limited. These  
345 nutrients stimulated soil microbial activity and enriched foliar N, and the effects were strongest



346 in nutrient-poor soil. These carcass-derived nutrient hotspots represent a previously unstudied  
347 function of megaherbivores on savannas – one that we need to better understand as  
348 megaherbivore populations continue to decline across their native ranges.

349

350 **Code Availability:** Computer code will be posted on Dryad Digital Repository.

351

352 **Data Availability:** Data will be archived on Dryad Digital Repository.

353

354 **Author Contributions:** Deron E. Burkepile, Nathan P. Lemoine, Izak P. J. Smit, Tercia  
355 Strydom, Aimee Tallian, Johan T. du Toit, Dave I. Thompson, and Joshua P. Schimel conceived  
356 the study. Michelle L. Budny, Johan T. du Toit, Nathan P. Lemoine, Joshua P. Schimel, Izak P.  
357 J. Smit, Tercia Strydom, Aimee Tallian, Dave I. Thompson, Helga van Coller, and Deron E.  
358 Burkepile collected samples. Courtney G. Reed, Nathan P. Lemoine, Dave I. Thompson, and  
359 Deron E. Burkepile analyzed the data. Courtney G. Reed drafted the manuscript, and all authors  
360 contributed to editing.

361

362 **Competing Interests:** The authors declare that they have no conflict of interest.

363

364 **Acknowledgments:** Funding for this research was provided by the National Science Foundation  
365 (#s 2128092, 2128093, and 2128094) and the University of California Santa Barbara Academic  
366 Senate. All research was completed under permits from South African National Parks (SS554).  
367 We thank the field assistants of SANParks for guiding and protection in the field, as well as the  
368 section rangers and Sandra Snelling for GPS locations and ages of carcasses.



369

370 **References**

- 371 1. Anderson, T. M., Hopcraft, J. G. C., Eby, S., Ritchie, M., Grace, J. B., & Olf, H. Landscape-  
372 scale analyses suggest both nutrient and antipredator advantages to Serengeti herbivore  
373 hotspots. *Ecol.*, 91, 1519–1529, <https://doi.org/10.1890/09-0739.1>, 2010.
- 374 2. Asner, G. P., Levick, S. R., Kennedy-Bowdoin, T., Knapp, D. E., Emerson, R., Jacobson, J.,  
375 Colgan, M. S., & Martin, R. E. Large-scale impacts of herbivores on the structural diversity  
376 of African savannas. *PNAS*, 106, 4947–4952, <https://doi.org/10.1073/pnas.0810637106>,  
377 2009.
- 378 3. Barton, P. S., Cunningham, S. A., Lindenmayer, D. B., & Manning, A. D. The role of carrion  
379 in maintaining biodiversity and ecological processes in terrestrial ecosystems. *Oecologia*,  
380 171, 761–772, <https://doi.org/10.1007/s00442-012-2460-3>, 2013.
- 381 4. Barton, P.S. Carrion Ecology, Evolution, and Their Applications. Edited by: M.E. Benbow,  
382 J.K. Tomberlin, A.M. Tarone. CRC Press, Boca Raton, FL, USA. 2016.
- 383 5. Barton, P. S., McIntyre, S., Evans, M. J., Bump, J. K., Cunningham, S. A., & Manning, A. D.  
384 Substantial long-term effects of carcass addition on soil and plants in a grassy eucalypt  
385 woodland. *Ecosphere*, 7, e01537, <https://doi.org/10.1002/ecs2.1537>, 2016.
- 386 6. Barton, P.S., Bump, J.K. Carrion decomposition. In: Carrion Ecology and Management.  
387 Edited by: P.P. Olea, P. Mateo-Tomas, J.A. Sanchez-Zapata. Springer, NY, USA, 101-124,  
388 2019.
- 389 7. Bates, D., Mächler, M., Bolker, B., & Walker, S. Fitting Linear Mixed-Effects Models Using  
390 lme4. *J. Stat. Softw.*, 67, 1–48, <https://doi.org/10.18637/jss.v067.i01>, 2015.



- 391 8. Britto, D. T., & Kronzucker, H. J. NH<sub>4</sub><sup>+</sup> toxicity in higher plants: a critical review. *J. Plant*  
392 *Physiol.*, 159, 567–584, <https://doi.org/10.1078/0176-1617-0774>, 2002.
- 393 9. Bump, J. K., Peterson, R. O., & Vucetich, J. A. Wolves modulate soil nutrient heterogeneity  
394 and foliar nitrogen by configuring the distribution of ungulate carcasses. *Ecol.*, 90, 3159–  
395 3167, <https://doi.org/10.1890/09-0292.1>, 2009.
- 396 10. Bump, J. K., Webster, C. R., Vucetich, J. A., Peterson, R. O., Shields, J. M., & Powers, M.  
397 D. (2009). Ungulate Carcasses Perforate Ecological Filters and Create Biogeochemical  
398 Hotspots in Forest Herbaceous Layers Allowing Trees a Competitive Advantage. *Ecosyst.*,  
399 12, 996–1007, <https://doi.org/10.1007/s10021-009-9274-0>, 2009.
- 400 11. Burnham, K. P. & Anderson, D. R. *Model Selection and Multimodel Inference*. Springer  
401 New York, NY. <http://doi.org/10.1007/b97636>, 2002.
- 402 12. Campos-Arceiz, A., & Blake, S. Megagardeners of the forest – the role of elephants in seed  
403 dispersal. *Acta Oecol.*, 37, 542–553, <https://doi.org/10.1016/j.actao.2011.01.014>, 2011.
- 404 13. Chen, J., Gutjahr, C., Bleckmann, A., & Dresselhaus, T. Calcium signaling during  
405 reproduction and biotrophic fungal interactions in plants. *Mol. Plant*, 8, 595–611,  
406 <https://doi.org/10.1016/j.molp.2015.01.023>, 2015.
- 407 14. Coe, M. The decomposition of elephant carcasses in the Tsavo (East) National Park, Kenya. *J.*  
408 *Arid Environ.*, 1, 71–86, [https://doi.org/10.1016/S0140-1963\(18\)31756-7](https://doi.org/10.1016/S0140-1963(18)31756-7), 1978.
- 409 15. Coetsee, M. & Ferreira, S. Bridging science, management, and opinion: GLTFCA elephant  
410 management [Conference presentation]. Savanna Science Network Meeting, Skukuza,  
411 Kruger National Park, South Africa, 2023 March 5-9.
- 412 16. Coverdale, T. C., Kartzinel, T. R., Grabowski, K. L., Shriver, R. K., Hassan, A. A., Goheen,  
413 J. R., Palmer, T. M., & Pringle, R. M. Elephants in the understory: opposing direct and



- 414 indirect effects of consumption and ecosystem engineering by megaherbivores. *Ecol.*, 97,  
415 3219–3230, <https://doi.org/10.1002/ecy.1557>, 2016.
- 416 17. Craine, J. M., Morrow, C., & Stock, W. D. Nutrient concentration ratios and co-limitation in  
417 South African grasslands. *New Phytol.*, 179, 829–836, <https://doi.org/10.1111/j.1469-8137.2008.02513.x>, 2008.
- 419 18. Danell, K., Berteaux, D., & Bråthen, K. A. Effect of Muskox Carcasses on Nitrogen  
420 Concentration in Tundra Vegetation. *Arctic*, 55, 389–392,  
421 <http://www.jstor.org/stable/40512497>, 2002.
- 422 19. Doughty, C. E., Roman, J., Faurby, S., Wolf, A., Haque, A., Bakker, E. S., Malhi, Y.,  
423 Dunning, J. B., Jr, & Svenning, J.-C. Global nutrient transport in a world of giants. *PNAS*,  
424 113, 868–873, <https://doi.org/10.1073/pnas.1502549112>, 2016.
- 425 20. Doughty, C. E., Wolf, A., & Malhi, Y. The legacy of the Pleistocene megafauna extinctions  
426 on nutrient availability in Amazonia. *Nat. Geosci.*, 6, 761–764,  
427 <https://doi.org/10.1038/ngeo1895>, 2013.
- 428 21. Flannery, T. F. Pleistocene faunal loss: implications of the aftershock for Australia’s past and  
429 future. *Archaeol. Ocean.*, 25, 45–55, <https://doi.org/10.1002/j.1834-4453.1990.tb00232.x>,  
430 1990.
- 431 22. Grant, C. C., & Scholes, M. C. The importance of nutrient hot-spots in the conservation and  
432 management of large wild mammalian herbivores in semi-arid savannas. *Biol. Conserv.*, 130,  
433 426–437, <https://doi.org/10.1016/j.biocon.2006.01.004>, 2006.
- 434 23. Guy, T. J., Hutchinson, M. C., Baldock, K. C. R., Kayser, E., Baiser, B., Staniczenko, P. P.  
435 A., Goheen, J. R., Pringle, R. M., & Palmer, T. M. Large herbivores transform plant-



- 436 pollinator networks in an African savanna. *Curr. Biol.*, 2964–2971,  
437 <https://doi.org/10.1016/j.cub.2021.04.051>, 2021.
- 438 24. Hocking, M. D. & Reynolds, J. D. Nitrogen uptake by plants subsidized by Pacific salmon  
439 carcasses: a hierarchical experiment. *Can. J. For. Res.*, 42, 908-917,  
440 <https://doi.org/10.1139/x2012-045>, 2012.
- 441 25. Holdo, R. M. Effects of fire history and N and P fertilization on seedling biomass, Specific  
442 Leaf Area, and root:shoot ratios in a South African savannah. *S. Afr. J. Bot.*, 86, 5–8,  
443 <https://doi.org/10.1016/j.sajb.2013.01.005>, 2013.
- 444 26. Hu, L., Wu, Z., Robert, C. A. M., Ouyang, X., Züst, T., Mestrot, A., Xu, J., & Erb, M. Soil  
445 chemistry determines whether defensive plant secondary metabolites promote or suppress  
446 herbivore growth. *PNAS*, 118, e2109602118, <https://doi.org/10.1073/pnas.2109602118>,  
447 2021.
- 448 27. Jobbágy, E. G., & Jackson, R. B. The uplift of soil nutrients by plants: Biogeochemical  
449 consequences across scales. *Ecol.*, 85, 2380–2389, <https://doi.org/10.1890/03-0245>, 2004.
- 450 28. Joern, A., Provin, T., & Behmer, S. T. Not just the usual suspects: insect herbivore  
451 populations and communities are associated with multiple plant nutrients. *Ecol.*, 93, 1002–  
452 1015, <https://doi.org/10.1890/11-1142.1>, 2012.
- 453 29. Kaspari, M. The Invisible Hand of the Periodic Table: How Micronutrients Shape Ecology.  
454 *Annu. Rev. Ecol. Evol. Syst.*, 52, 199–219, [https://doi.org/10.1146/annurev-ecolsys-012021-  
455 090118](https://doi.org/10.1146/annurev-ecolsys-012021-090118), 2021.
- 456 30. Keenan, S. W., & Beeler, S. R. Long-term effects of buried vertebrate carcasses on soil  
457 biogeochemistry in the Northern Great Plains. *PloS One*, 18, e0292994,  
458 <https://doi.org/10.1371/journal.pone.0292994>, 2023.



- 459 31. Lemoine, N. P., Budny, M. L., Rose, E., Lucas, J., & Marshall, C. W. Seasonal soil moisture  
460 thresholds inhibit bacterial activity and decomposition during drought in a tallgrass prairie.  
461 *Oikos*, 2024, e10210, <https://doi.org/10.1111/oik.10201>, 2024.
- 462 32. Macdonald, B. C. T., Farrell, M., Tuomi, S., Barton, P. S., Cunningham, S. A., & Manning,  
463 A. D. Carrion decomposition causes large and lasting effects on soil amino acid and peptide  
464 flux. *Soil Biol. Biochem.*, 69, 132–140, <https://doi.org/10.1016/j.soilbio.2013.10.042>, 2014.
- 465 33. Monk, J. D., Donadio, E., Smith, J. A., Perrig, P. L., Middleton, A. D., & Schmitz, O. J.  
466 Predation and Biophysical Context Control Long-Term Carcass Nutrient Inputs in an Andean  
467 Ecosystem. *Ecosyst.*, 27, 346–359, <https://doi.org/10.1007/s10021-023-00893-7>, 2024.
- 468 34. Mphopya, J. N., Galy-Lacaux, C., Lacaux, J. P., Held, G., & Pienaar, J. J. Precipitation  
469 Chemistry and Wet Deposition in Kruger National Park, South Africa. *J. Atmos. Chem.*, 53,  
470 169–183, <https://doi.org/10.1007/s10874-005-9005-7>, 2006.
- 471 35. Oksanen J, Simpson G, Blanchet F, Kindt R, Legendre P, Minchin P, O'Hara R, Solymos P,  
472 Stevens M, Szoecs E, Wagner H, Barbour M, Bedward M, Bolker B, Borcard D, Carvalho G,  
473 Chirico M, De Caceres M, Durand S, Evangelista H, FitzJohn R, Friendly M, Furneaux B,  
474 Hannigan G, Hill M, Lahti L, McGlenn D, Ouellette M, Ribeiro Cunha E, Smith T, Stier A,  
475 Ter Braak C, Weedon J. Community Ecology Package. R package version 2.6-4,  
476 <https://CRAN.R-project.org/package=vegan>, 2022.
- 477 36. Olea, P.P, Mateo-Tomas, P., Sanchez-Zapata, J.A. (eds.) Carrion Ecology and Management.  
478 Springer, NY, USA, 2019.
- 479 37. Owen-Smith, N. Megafaunal extinctions: the conservation message from 11,000 years B.P.  
480 *Conserv. Biol.*, 3, 405–412, <https://www.jstor.org/stable/2386221>, 1989.



- 481 38. Owen-Smith, N., & Mills, M. G. L. Predator-prey size relationships in an African large-  
482 mammal food web. *J. Anim. Ecol.*, 77, 173–183, [https://doi.org/10.1111/j.1365-](https://doi.org/10.1111/j.1365-2656.2007.01314.x)  
483 [2656.2007.01314.x](https://doi.org/10.1111/j.1365-2656.2007.01314.x), 2008.
- 484 39. Pandey, N. Role of Micronutrients in Reproductive Physiology of Plants.  
485 <https://www.semanticscholar.org/paper/af9a8662b83613f6e0d5e538ed33f3add4a1d5a1>,  
486 2010.
- 487 40. Parmenter, R. R., & MacMahon, J. A. Carrion decomposition and nutrient cycling in a  
488 semiarid shrub–steppe ecosystem. *Ecol. Monogr.*, 79, 637–661, [https://doi.org/10.1890/08-](https://doi.org/10.1890/08-0972.1)  
489 [0972.1](https://doi.org/10.1890/08-0972.1), 2009.
- 490 41. Pellegrini, A. F. A. Nutrient limitation in tropical savannas across multiple scales and  
491 mechanisms. *Ecol.*, 97, 313–324, <https://doi.org/10.1890/15-0869.1>, 2016.
- 492 42. Prosser, J. I. Soil Nitrifiers and Nitrification. In *Nitrification*. ASM Press, pp. 347-383, 2014.
- 493 43. Quaggiotto, M.-M., Evans, M. J., Higgins, A., Strong, C., & Barton, P. S. Dynamic soil  
494 nutrient and moisture changes under decomposing vertebrate carcasses. *Biogeochemistry*,  
495 146, 71–82, <https://doi.org/10.1007/s10533-019-00611-3>, 2019.
- 496 44. R Core Team. R: A language and environment for statistical computing. R Foundation for  
497 Statistical Computing, Vienna, Austria. <https://www.R-project.org/>, 2022.
- 498 45. Ries, L. P., & Shugart, H. H. Nutrient limitations on understory grass productivity and  
499 carbon assimilation in an African woodland savanna. *J. Arid Environ.*, 72, 1423–1430,  
500 <https://doi.org/10.1016/j.jaridenv.2008.02.013>, 2008.
- 501 46. Ripple, W. J., Newsome, T. M., Wolf, C., Dirzo, R., Everatt, K. T., Galetti, M., Hayward, M.  
502 W., Kerley, G. I. H., Levi, T., Lindsey, P. A., Macdonald, D. W., Malhi, Y., Painter, L. E.,





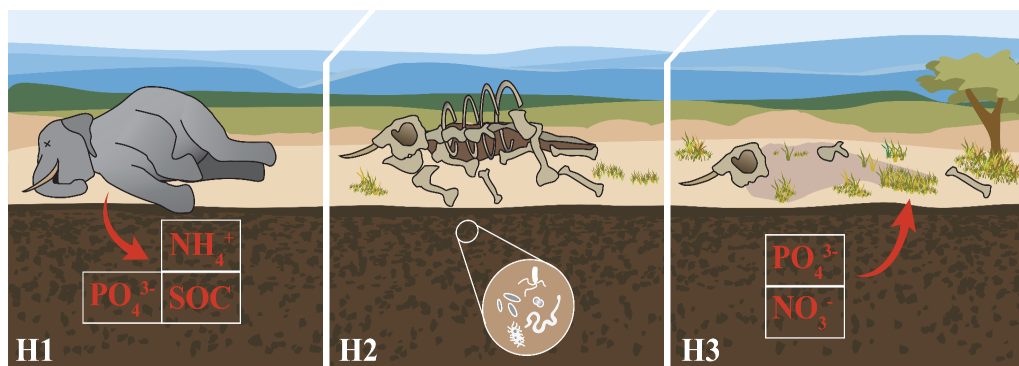
- 503 Sandom, C. J., Terborgh, J., & Van Valkenburgh, B. Collapse of the world's largest  
504 herbivores. *Sci. Adv.*, 1, e1400103, DOI:[10.1126/sciadv.1400103](https://doi.org/10.1126/sciadv.1400103), 2015.
- 505 47. Risch, A. C., Frossard, A., Schütz, M., Frey, B., Morris, A. W., & Bump, J. K. Effects of elk  
506 and bison carcasses on soil microbial communities and ecosystem functions in Yellowstone,  
507 USA. *Funct. Ecol.*, 34, 1933–1944, <https://doi.org/10.1111/1365-2435.13611>, 2020.
- 508 48. Roman, J., Estes, J. A., Morissette, L., Smith, C., Costa, D., McCarthy, J., Nation, J. B.,  
509 Nicol, S., Pershing, A., & Smetacek, V. Whales as marine ecosystem engineers. *Front. Ecol.*  
510 *Environ.*, 12, 377–385, <https://doi.org/10.1890/130220>, 2014.
- 511 49. Sardans, J., & Peñuelas, J. Potassium Control of Plant Functions: Ecological and Agricultural  
512 Implications. *Plants*, 10, <https://doi.org/10.3390/plants10020419>, 2021.
- 513 50. Schmitz, O. J., Wilmers, C. C., Leroux, S. J., Doughty, C. E., Atwood, T. B., Galetti, M.,  
514 Davies, A. B., & Goetz, S. J. Animals and the zoogeochemistry of the carbon cycle. *Science*,  
515 362, <https://doi.org/10.1126/science.aar3213>, 2018.
- 516 51. Skarpe, C., Aarrestad, P. A., Andreassen, H. P., Dhillion, S. S., Dimakatso, T., du Toit, J. T.,  
517 Duncan, Halley, J., Hytteborn, H., Makhabu, S., Mari, M., Marokane, W., Masunga, G.,  
518 Ditshoswane, M., Moe, S. R., Mojaphoko, R., Mosugelo, D., Motsumi, S., Neo-Mahupeleng,  
519 G., ... Wegge, P. The return of the giants: ecological effects of an increasing elephant  
520 population. *Ambio*, 33, 276–282, <http://www.jstor.org/stable/4315497>, 2004.
- 521 52. Sterner, R. W., & Elser, J. J. *Ecological Stoichiometry: The Biology of Elements from*  
522 *Molecules to the Biosphere*. Princeton University Press.  
523 <http://www.jstor.org/stable/j.ctt1jkrp3>, 2002.



- 524 53. Subalusky, A. L., Dutton, C. L., Rosi, E. J., & Post, D. M. Annual mass drownings of the  
525 Serengeti wildebeest migration influence nutrient cycling and storage in the Mara River.  
526 PNAS, 114, 7647–7652, <https://doi.org/10.1073/pnas.1614778114>, 2017.
- 527 54. Subalusky, A.L., Dutton, C.L., Rosi, E.J., Puth, L.M., Post, D.M. River of bones: wildebeest  
528 skeletons leave a legacy of mass mortality in Mara River, Kenya. *Front. Ecol. Evol.*, 8,  
529 <https://doi.org/10.3389/fevo.2020.00031>, 2020.
- 530 55. Towne, E. G. Prairie vegetation and soil nutrient responses to ungulate carcasses. *Oecologia*,  
531 122, 232–239, <https://www.jstor.org/stable/4222536>, 2000.
- 532 56. Turner, W. C., Kausrud, K. L., Krishnappa, Y. S., Cromsigt, J. P. G. M., Ganz, H. H.,  
533 Mapaure, I., Cloete, C. C., Havarua, Z., Küsters, M., Getz, W. M., & Stenseth, N. C. Fatal  
534 attraction: vegetation responses to nutrient inputs attract herbivores to infectious anthrax  
535 carcass sites. *Proc. R. Soc. B*, 281, <https://doi.org/10.1098/rspb.2014.1785>, 2014.
- 536 57. van Klink, R., van Laar-Wiersma, J., Vorst, O., & Smit, C. Rewilding with large herbivores:  
537 Positive direct and delayed effects of carrion on plant and arthropod communities. *PloS One*,  
538 15, e0226946, <https://doi.org/10.1371/journal.pone.0226946>, 2020.
- 539 58. Venter FJ, Scholes RJ, Eckhardt HC. Abiotic template and its associated vegetation pattern.  
540 In: JT Du Toit, KH Rogers, HC Biggs, eds. *The Kruger experience: ecology and*  
541 *management of savanna heterogeneity*. Washington, DC, USA: Island Press, 83–129, 2003.
- 542 59. Wiersum, L. K. Uptake of nitrogen and phosphorus in relation to soil structure and nutrient  
543 mobility. *Plant Soil*, 16, 62–70, <https://doi.org/10.1007/BF01378158>, 1962.
- 544 60. Yang, L. H. Periodical cicadas as resource pulses in North American forests. *Science*, 306,  
545 1565–1567, <https://doi.org/10.1126/science.1103114>, 2004.

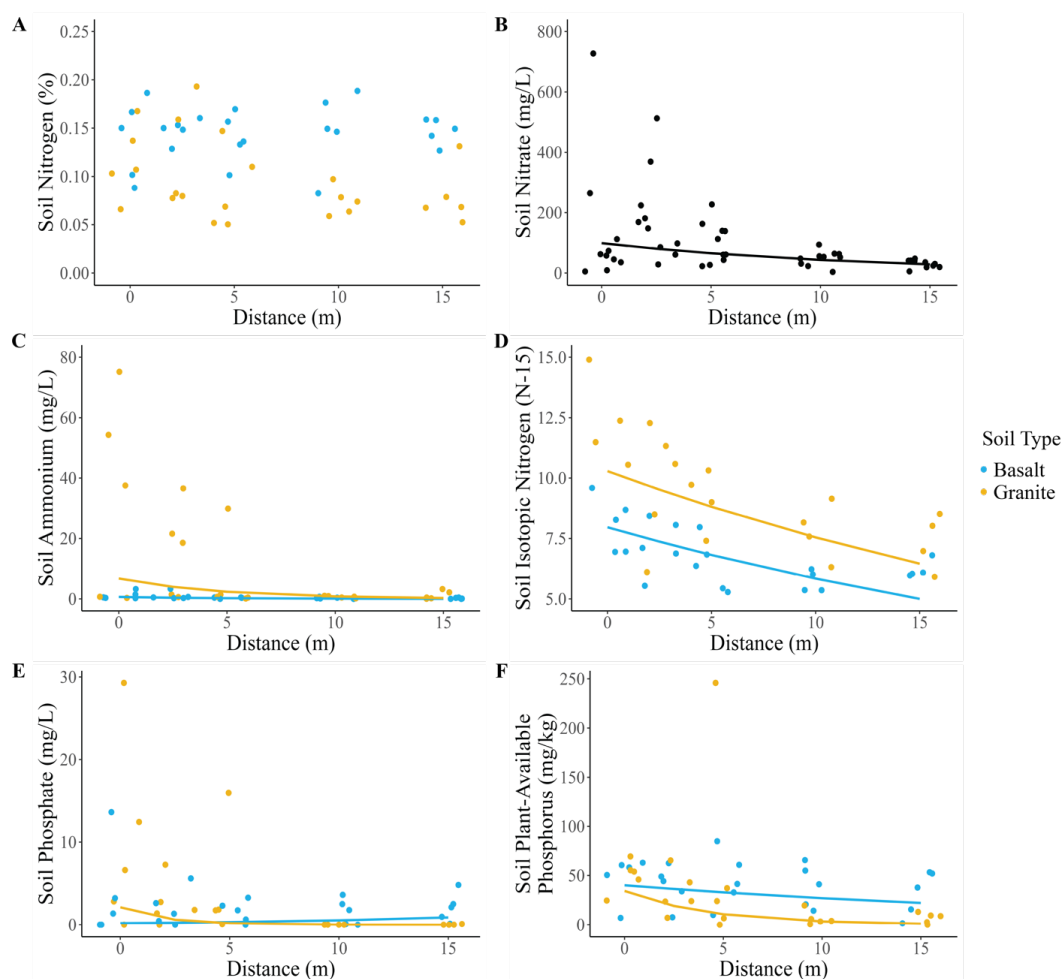


- 546 61. Yang, L. H. Pulses of dead periodical cicadas increase herbivory of American bellflowers.  
547 Ecol., 89, 1497–1502, <https://doi.org/10.1890/07-1853.1>, 2008.
- 548 62. Yong, S. K., Jalaludin, N. H., Brau, E., Shamsudin, N. N., & Heo, C. C. Changes in soil  
549 nutrients (ammonia, phosphate and nitrate) associated with rat carcass decomposition under  
550 tropical climatic conditions. Soil Res., 57, 482–488, <https://doi.org/10.1071/SR18279>, 2019.  
551



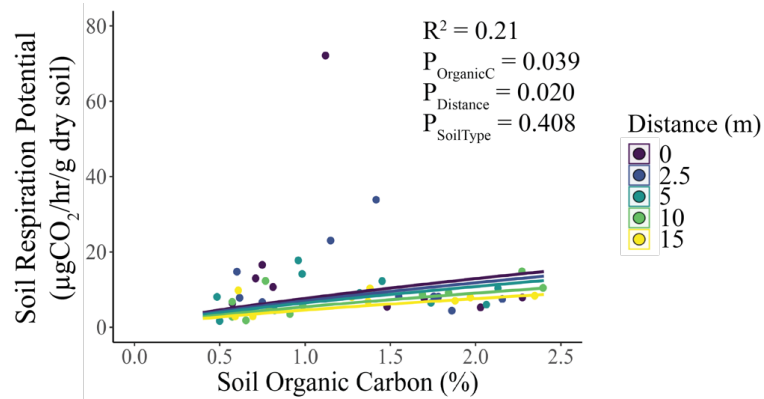
552

553 **Figure 1.** Hypothesized impacts of elephant megacarcasses on soil and plant nutrients. First  
554 (H1), we hypothesized that elephant carcasses would release pulses of nutrients into the soil,  
555 resulting in higher concentrations of soil nutrients such as nitrogen (ammonium,  $[\text{NH}_4]^+$ ),  
556 phosphorus (phosphate,  $[\text{PO}_4]^{3-}$ ), and soil organic C. Second (H2), we hypothesized that C inputs  
557 from the carcass would result in increased soil microbial respiration potential. Third (H3), we  
558 hypothesized that plants would take up nutrients from the carcass soil, resulting in plants with  
559 distinct nutrient profiles and increased concentrations of key limiting nutrients such as N and P.  
560 Image credit: Kirsten Boeh.



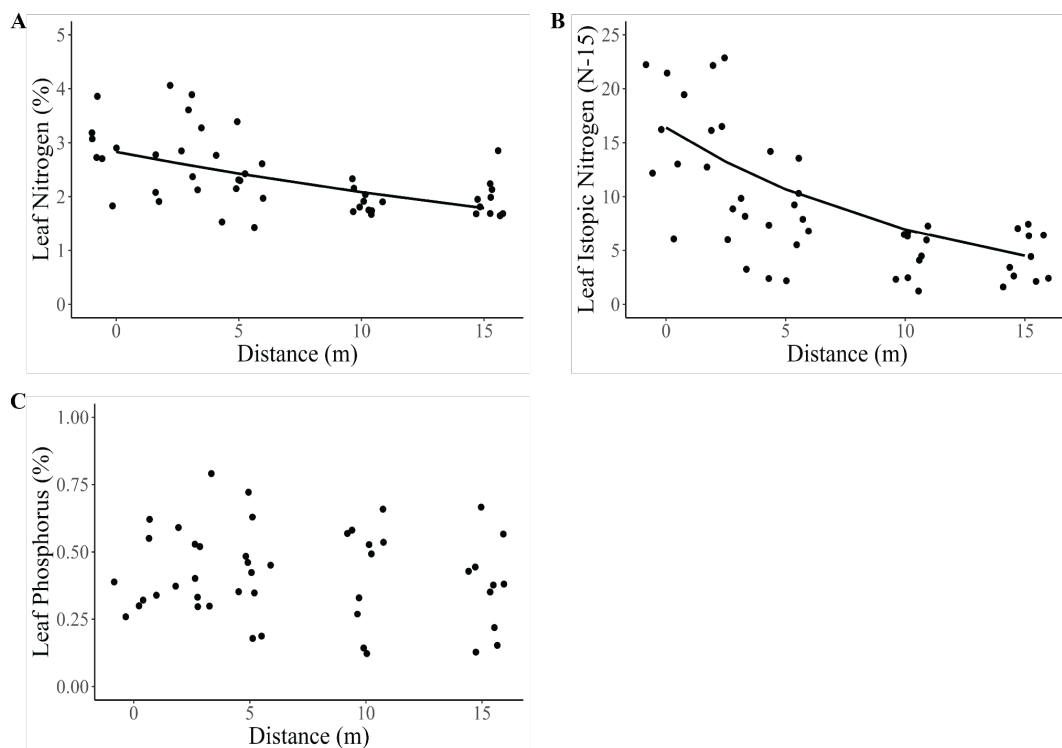
561

562 **Figure 2.** Soil N and P responses to elephant carcasses. (A) Soil N (%) was greater in basaltic  
 563 soils but did not differ with distance from the center of the carcass site. (B) Soil nitrate decreased  
 564 with distance but did not differ with soil type. (C) Ammonium and (D) <sup>15</sup>N were both greater in  
 565 granitic soils and decreased with distance from the carcass. (E) Soil phosphate and (F) plant-  
 566 available P both decreased with distance, and the effects were stronger in granitic soils. Log-  
 567 transformed data have been back-transformed for visualization. Points represent individual  
 568 measurements and are offset to be visible when they would otherwise overlap. Each plot includes  
 569 only visualization (i.e., lines/colors) for parameters that were included in the set of top models.



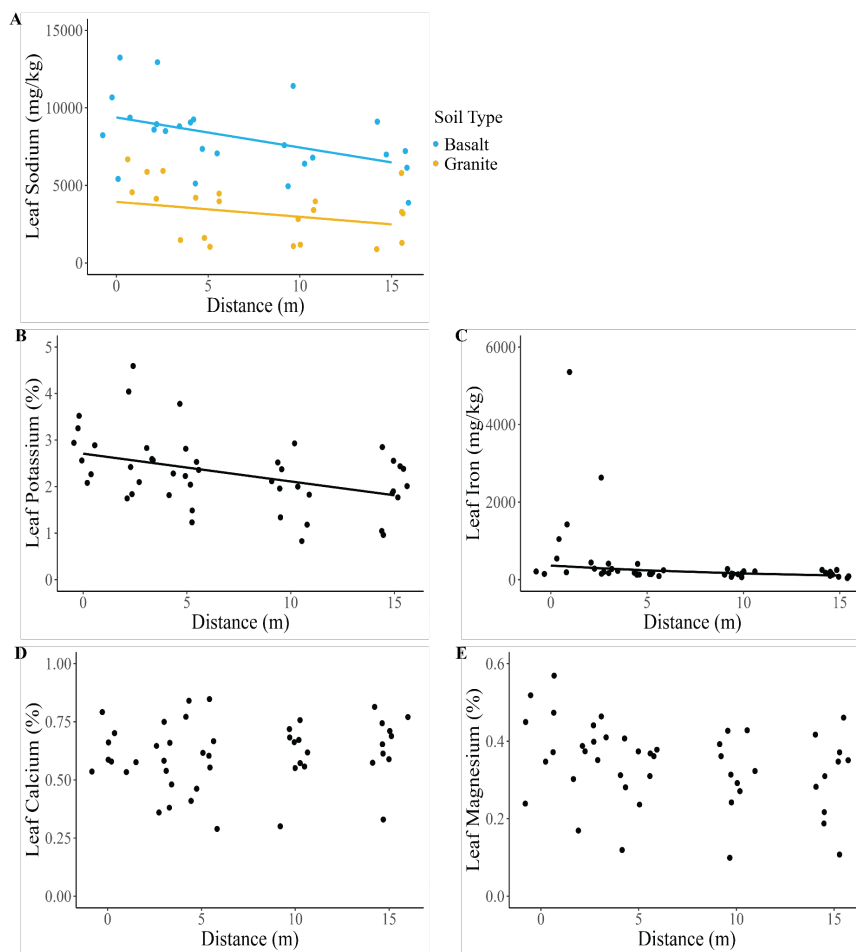
570

571 **Figure 3.** Soil respiration potential was positively correlated with soil organic C (%) and  
572 decreased significantly with distance from the carcass. Log-transformed data have been back-  
573 transformed for visualization. Points represent individual measurements and are offset to be  
574 visible when they would otherwise overlap.



575

576 **Figure 4.** Leaf N and P responses to elephant carcasses. (A) Leaf %N and (B)  $^{15}\text{N}$  both  
577 decreased with distance from the carcass site, while (C) leaf P did not differ significantly with  
578 distance or soil type. Log-transformed data have been back-transformed for visualization. Points  
579 represent individual measurements and are offset to be visible when they would otherwise  
580 overlap. Three of the ten sites had bare ground at the 0 m distance, resulting in a sample size of 7  
581 sites for that distance and 10 for the other distances.



582

583 **Figure 5.** Generalized linear mixed model results for leaf micronutrients. (A) Leaf Na was  
584 greatest in basaltic soil and decreased significantly with distance. (B) Leaf K and (C) Fe both  
585 decreased significantly with distance. (D) Ca and (E) Mg did not differ significantly with  
586 distance or soil type. Log-transformed data have been back-transformed for visualization. Points  
587 represent individual measurements and are offset to be visible when they would otherwise  
588 overlap.